Explore Stochastic Instabilities of Periodic Points by Transition Path Theory

Yu Cao[1], Ling Lin[*2], Xiang Zhou[†1],

[1] Department of Mathematics, City University of Hong Kong,
Tat Chee Ave, Kowloon, Hong Kong.
[2] Institute for Mathematics, Freie Universität Berlin,
Arnimallee 6, 14195 Berlin, Germany.

January 8, 2016

arXiv:1601.01424v1 [nlin.CD] 7 Jan 2016

Abstract. We consider the noise-induced transitions in the randomly perturbed discrete logistic map from a linearly stable periodic orbit consisting of T periodic points. The traditional large deviation theory and asymptotic analysis for small noise limit as well as the derived quasi-potential can not distinguish the quantitative difference in noise-induced stochastic instabilities of these T periodic points. We generalize the transition path theory to the discrete-time continuous-space stochastic process to attack this problem. As a first criterion of quantifying the relative instability among T periodic points, we compare the distribution of the last passage locations in the transitions from the whole periodic orbit to a prescribed set far away. This distribution is related to the contributions to the transition rate from each periodic points. The second criterion is based on the competency of the transition paths associated with each periodic point. Both criteria utilise the reactive probability current in the transition path theory. Our numerical results for the logistic map reveal the transition mechanism of escaping from the stable periodic orbit and identify which periodic point is more prone to lose stability so as to make successful transitions under random perturbations.

Key words and phrases: random logistic map, transition path theory, periodic orbit, stochastic instability

1. Introduction

When deterministic dynamical systems are perturbed by random noise, even though the noise amplitude is small, it has a prominent influence on the dynamics on the appropriate time-scale. For example, the thermal noise can induce important physical and biological metastability phenomena such as phase transitions, nucleation events, configuration changes of macromolecules. These phenomena correspond to the very unlikely excursions in the phase space of the random trajectories, so these events are usually called *rare events*. These trajectories have to overcome some barriers to escape from the initial metastable state and enter

[*]L. Lin acknowledges the financial support of the DRS Fellowship Program of Freie Universität Berlin.

[†]Corresponding author. email: *xiang.zhou@cityu.edu.hk*. X. Zhou acknowledges the financial support of Hong Kong GRF (109113,11304314,11304715).

Date: January 8, 2016.

another. For the understanding of the occurrence of rare events, it is of great importance to investigate the non-equilibrium statistical and dynamical behaviours of those trajectories successfully making transitions. One of the interesting questions is how the ensemble of these transition trajectories depend on the phase space of the unperturbed deterministic dynamical systems, for example, what structure in the phase space would be the barriers for transitions, how the system leaves the initial metastable state and escapes the basin of attraction of this metastable state, etc. For general dynamics, the metastable state may not be a single point as a local minimum on potential energy surface; it may be a collection of points, such as limit cycle, periodic orbit, or even chaotic attractor. In this paper, we are interested in, conditioned on the occurrence of rare transitions from one of these stable structures, through which location *within* the metastable set the transition trajectories will leave with a higher or dominant probability. Particularly, as an example, our study focuses on the stable periodic orbits in the randomly perturbed logistic map.

In history, many research work target to explore the barrier on the basin boundary. For the diffusion process on a potential energy surface (a classic model for chemical reactions [1,2]), the well-known transition-state theory [3] states that basically the transition state, is a saddle point with index 1 on the potential energy surface. The progresses of chemical reactions are mainly described by heteroclinic orbits connecting the local minima through the saddle point, i.e., "minimum energy path". In addition, one can calculate the transition rate by computing the probability flux of particles that cross the dividing surface of two neighbouring potential wells. For general continuous time dynamical systems under random perturbations, the notion of "most probable path" is very useful to describe the transition process. This path is a curve in the phase space with a dominant contribution in the ensemble of transition trajectories at vanishing noise limit. From a mathematical viewpoint, such a notion of most probable path is based on the large deviation principle (LDP) in path space. The well-known Freidlin-Wentzell theory [4] states that the most probable transition path from one set A to another B is the *minimum action path*, which minimizes the rate function of the Freidlin-Wentzell LDP (aka."Freidlin-Wentzell action functional") subject to the constraint of starting from A and ending at B. The transition probability is dominated by the minimal value of the rate function. Therefore, by analytically performing asymptotic analysis such as WKB or instanton analysis [5–8], or numerically solving the variational problem in a path space [9–11], one can identify most probable escape/transition path. This allows a further examination of the path and the unstable structure in the phase space, in particular, how this path crosses the basin boundaries. This methodology of least action principle is applicable for general dynamical systems of continuous-time or discrete-time. The applications to Lorenz model [12], Kuramoto-Sivashinsky PDE [13] have already discovered the barriers on the basin boundary in types of saddle points or saddle cycles.

For discrete maps perturbed by noise, there has been a long history of studying the effect of random perturbations on the dynamics. Some works are based on the brute-force simulation to collect the empirical distributions of transition trajectories [14]. The applications of the large deviation rate function in the setting of

discrete-time maps included the work in [15, 16] which studied the transitions between stable fixed points, stable periodic orbits and chaotic attractors, providing empirical evidence that the transition state is the type of a saddle node. [17, 18] focused on the *quasi-potential* (activation energy), which is a good quantification of the stochastic stability for a metastable set, to investigate the key invariant set on the basin boundary. The series work of [19–21] carried extensive studies for Lorenz systems, Henon maps and other examples of discrete maps under additive random perturbation. Their results seem to suggest that in the noise-induced escape from the basin of attraction of a stable set, the barrier-crossing on the basin boundary is mostly determined by the position and stability properties of certain saddle point or saddle cycles. Recently, a new approach was developed in [22, 23] to understand transport in stochastic dynamical systems. They basically use the transition probability matrix (after discretizing and reindexing the continuous space) for identification of active regions of stochastic transport. Most of these existing studies deal with the transition state (or the set) on the basin of attraction of a metastable state (or invariant set).

In this paper, we are interested in the transition from set to set with the purpose of pinpointing the role of individual points in the initial metastable set to escape. The motivation comes from the questions below: how the randomly perturbed system leaves the periodic orbit (or limit cycle in continuous time dynamics); how the stable self-sustained oscillating motion is eventually destroyed by the noise.

Specifically, we consider the random logistic map with additive Gaussian noise. We are concerned with the noise-induced transitions from A to B — two disjoint sets in the phase space. It is assumed that the unperturbed system has a linearly stable periodic orbit (all eigenvalues are less than one in modulus), denoted as $\boldsymbol{\xi} = (\xi_1, \xi_2, \cdots, \xi_T)$, where the integer T is the period. To explore the stochastic instability of $\boldsymbol{\xi}$, we select A as the union of the T periodic points $\{\xi_i\}$ (more precisely, A is the union of T small windows around $\{\xi_i\}$. Refer to Section 2). After an exponentially long time wandering around the metastable set A in the random motion of nearly periodic oscillation, the stochastic system will eventually get a chance of making a significant transition to a set B far away from A. The question we shall address is how the system deviates from the typical periodic oscillation and whether it have any preference to some special periodic points to make the transition.

The traditional techniques based on large deviation principle and the concept of quasi-potential are not capable of addressing the above question due to the following fact, although they are quite successful in studying the most active regions on the basin boundary of the set A. If the unperturbed deterministic flow can go from a point x to another point y, then the cost (quasi-potential) from x to y is simply zero. Thus, if any points in the set A can reach each other mutually by the deterministic flow (periodic orbit or limit cycle certainly satisfies this condition), then the quasi-potential is flat on the whole set A. From any point in A, the minimal action to escape the basin is the same. The extremal path minimizing the action functional usually takes infinite time and has infinitely length, and the whole invariant set A is the α-limit set of the extremal path: There is no particular location in the set A from where the extremal path emits. Hence, the action functional and the minimum action path can not distinguish individual

points inside A in such cases. Similarly, the singular perturbation method [24] for the mean first passage time in the vanishing noise limit will give a constant value of the WKB solution on the stable limit cycle, and thus may be not directly useful to our problem.

We use a new and attractive tool, the transition path theory [25–28], by modifying this theory for the discrete map. The transition path theory for continuous-time dynamical systems has been proved to be an effective mathematical tool to reveal transition mechanism of a few complex physical and biological systems [29,30]. This article intends to bring the transition path theory into studying the stochastic instability issues for random discrete maps. We shall formulate the transition path theory for the discrete-time continuous-space Markov process. We then use three key ingredients in the transition path theory, the reactive current, the transition rate and the dominant transition path, to understand the escape mechanism from the periodic orbit A for any finite noise. To quantitatively compare the stochastic instability of the T individual periodic points, we propose two rules: the first one is the distribution of the last passage position among these T point and the second one is the starting point of the dominant transition path. Our numerical results obtained clearly show the capability of this theory in quantitative understanding of the different roles of the individual points belonging to the same periodic orbit.

The paper is organized as follows. In Section 2, we will set up our problem for the random logistic map. In Section 3, we briefly review the existing methodologies. Section 4 is our method based on the transition path theory. In section 5, we present numerical results for the random logistic map. Section 6 is our concluding discussion.

2. Random Logistic Map

The randomly perturbed discrete map of our interest is the following

$$x_{n+1} = F(x_n) + \sigma\eta_n$$

where $\eta_n \sim N(0,1)$ are *i.i.d.* standard normal random variables and the constant $\sigma > 0$ is the noise amplitude. In this paper, we focus on a well-known example of F: the logistic map. Logistic map is probably the simplest nonlinear mapping giving rise to periodic and chaotic behaviors. It is popularly used as a discrete-time demographic model to represent the population with density-dependent mortality. Mathematically, the logistic map is written by

$$x \to F(x) := \alpha x(1-x),$$

where x is a number between zero and one that represents the ratio of existing population to the maximum possible population. $\alpha > 0$ is the parameter. When x is out of the interval $[0,1]$, the logistic map simply diverges to infinity and never returns. The dynamics of interest is in the interval $[0,1]$. There are two fixed points in this interval, 0 and $1-\frac{1}{\alpha}$. When $0<\alpha<1$, 0 is the only stable fixed point and when $1<\alpha<3$, $1-\frac{1}{\alpha}$ is the only stable fixed point. Both fixed points become unstable for α larger than 3. $\alpha = 3$ is the onset of a stable period-2 orbit, and this period-2 orbit disappears at $\alpha = 1+\sqrt{6} \approx 3.4495$, at which the period-4 orbit takes over. The stable period-2^n orbit is followed by the stable period-2^{n+1} orbit if α increases continuously. This phenomenon is termed as period doubling cascade and leads to the onset of chaos. Apart from this, tangent bifurcation is

found, e.g., the onset of stable period-3 orbit arises at $\alpha = 1 + 2\sqrt{2} \approx 3.828$. Further details about the logistic map can be found in some classic literature, e.g., [31].

The random logistic map of our interest is the following additive random perturbation restricted on the interval $D = [0, 1]$ with $F(x) = \alpha x(1 - x)$:

$$x_{n+1} = F(x_n) + \sigma\eta_n \mod 1. \tag{2.1}$$

We here impose the periodic boundary condition for the Markov process $\{x_n\}$ so that all dynamics is restricted on the compact set D. This will guarantee the unique existence of the invariant measure for $\{x_n\}$ on D and thus ergodicity holds for this stochastic process, which is a fundamental assumption in the transition path theory. Other type of boundary condition is also feasible such as the reflection boundary condition at $x = 0$ and $x = 1$.

The transition probability density of the discrete-time continuous-space Markov process (2.1) is

$$P(x, y) = \sum_{l\in\mathbb{Z}} \frac{1}{\sqrt{2\pi\sigma^2}} \exp\left(-\frac{1}{2\sigma^2}(y - F(x) + l)^2\right), \tag{2.2}$$

where the sum over the integer l is merely a minor adjustment for the periodic boundary condition we used here. The density of the unique invariant measure, $\pi(x)$, is the solution of the following balance equation

$$\int_D P(y, x)\pi(y)\,\mathrm{d}y = \pi(x). \tag{2.3}$$

In other words, $\pi(x)$ is the eigenfunction for the principle eigenvalue of the adjoint of the transition kernel $P(x, y)$.

Now we specify the sets involved in the transition problems for the randomly perturbed logistic map. The parameter α in our study will be selected so that the logistic map only has periodic oscillations. The stable invariant set of interest here is the (linearly) stable period-T orbit in the (unperturbed) logistic map, denoted as $\boldsymbol{\xi} = (\xi_1, \xi_2, \cdots, \xi_T)$. The order of (ξ_i) in $\boldsymbol{\xi}$ is specified so that $\xi_{i+1} = F(\xi_i)$. We pick a small neighbourhood A around the T periodic points and a disjoint set B. With these setups, the noise-induced transitions from A to B, named as A-B transitions, will be our focus. By specifying the width δ_a, the set A around the periodic orbit $\boldsymbol{\xi}$ is the union of the T disjoint small windows

$$A = \bigcup_{1\le i\le T} [\xi_i - \delta_a, \xi_i + \delta_a]. \tag{2.4}$$

It is possible to specify different widths for different periodic points, or let the interval be asymmetric around ξ_i. It is also possible to use the level set of the invariant measure π, $\{x : \pi(x) < \delta\}$, around the periodic points. In the study of this paper, we use the same δ_a for simplicity. The set B is placed near the unstable fixed point 0 (or 1) with the width δ_b:

$$B = [0, \delta_b] \cup [1 - \delta_b, 1]. \tag{2.5}$$

δ_a and δ_b are small enough so that $A \cap B = \emptyset$ and $[\xi_i - \delta_a, \xi_i + \delta_a] \cap [\xi_j - \delta_a, \xi_j + \delta_a] = \emptyset$ is empty for any $1 \le i < j \le T$. The set B in our logistic map example is around the unstable point, the "furthest" boundary point from the stable set A. In general situations, this set B is placed just outside the basin of attraction of the periodic

orbit $\boldsymbol{\xi}$ and the instability result about the $\boldsymbol{\xi}$ is typically robust for small noise amplitude.

We introduce the nonzero width δ_a for the periodic orbit $\boldsymbol{\xi}$, because the space is continuous, not discrete: it makes no sense to consider trajectories in stochastic system exactly leaving or entering some singleton points, at a fixed noise amplitude $\sigma > 0$. In practice, the specification of the window width δ_a should be given by the user who decides to what extent the system is deemed as out of the oscillation status for specific applications.

Usually, the width δ_a should be small enough so that the set A_i can represent the transition behaviour for the point ξ_i inside. In theory, for a set A to truly reflect the transition mechanism of escaping from $\boldsymbol{\xi}$, the width δ_a should approach zero. In fact, all calculations are based on a finite δ_a. But since the set A has the metastability property (linearly stable), then it follows that the conclusions to our question based on the study of the set A for finitely small δ_a are quite robust and indeed give correct insights about the transition mechanisms and the stochastic instabilities for the stable periodic orbit $\boldsymbol{\xi}$.

3. Related Works

We first briefly review two existing methods for the study of stochastic systems. The known applications of both methods are mainly for exploring the basin boundary.

3.1. **Large deviation principle.** We give a glimpse of the large deviation principle (LDP) or the principle of least action for randomly perturbed discrete map. For continuous-time diffusions processes, refer to the Freidlin-Wentzell theory in [4]. We start from the transition probability for the random mapping $x_{n+1} = F(x_n) + \sigma\eta_n$, which is

$$P(x, y) = \frac{1}{\sqrt{2\pi\sigma^2}} \exp\left(-\frac{(y - F(x))^2}{2\sigma^2}\right).$$

With the fixed initial point x_0 at time 0 and ending point x_n at time n, the probability of a path $\boldsymbol{\gamma} = (x_0, x_1, \cdots, x_{n-1}, x_n)$ is

$$P[\boldsymbol{\gamma}] = \prod_{i=0}^{n-1} p(x_i, x_{i+1}) \propto Z_\sigma^{-1} \exp\left(-\frac{1}{\sigma^2} S[x_0, \cdots, x_n]\right), \tag{3.1}$$

where Z_σ^{-1} is the prefactor and the cost function S has the form of

$$S[\boldsymbol{\gamma}] = S[x_0, \cdots, x_n] = \frac{1}{2}\sum_{i=0}^{n-1}(x_{i+1} - F(x_i))^2. \tag{3.2}$$

This cost function S is actually the *rate function* (aka. action) of the LDP at the vanishing noise limit $\sigma \downarrow 0$. By the Laplace's method, the path probability $P[\boldsymbol{\gamma}]$ is asymptotically dominated by $\exp\left(-\frac{1}{\sigma^2} S_{\min}\right)$, where $S_{\min} = \min_\gamma S[\boldsymbol{\gamma}]$. The *minimum action path* (MAP) $\boldsymbol{\gamma}^*$ is the one such that $S[\boldsymbol{\gamma}^*] = S_{\min}$. If this minimal action $S_{\min}$ is viewed as the function of the initial point x_0 and the ending point x_n for all possible n, then it is the so-called *quasi-potential*, which is quite useful for quantifying the stability of each basin against the random perturbation [4, 15, 32]. When the initial point x_0 is in a stable structure (fixed point, periodic orbit,

chaotic attractor) of the phase space, and x_n is out of the basin of attraction of this stable structure, the MAP is usually called the *most probable escape path* (MPEP). The intersection part of the MPEP with the basin boundary is quite revealing for transition states or active regions during crossing the boundary.

One obvious feature of this least action method based on the LDP is that the cost is *zero* for a path from ξ_1 to ξ_2 if ξ_2 is exactly equal to $F(\xi_1)$. This means that starting from any point in the same period-T orbit, the minimal action is the same. Thus, one can not tell which point in the periodic orbit, limit cycle, or even chaotic attractor, is more prone to the random perturbation, since they share the same action.

3.2. **PDF flux.** To study the bi-stabilities in the stochastically perturbed dynamical systems, Billings *et al.* [22, 23] proposed a method on the transport of probability density function under the discrete map, in which the one-step transport is described by the Frobenius-Perron operator, i.e., the adjoint of the transition kernel $P(x, y)$. They investigated how an initial distribution is transported to a given region in the phase space under the action of this operator:

$$\rho(x) \to \mathcal{F}[\rho](x) := \int_D P(y, x)\rho(y)\,\mathrm{d}y.$$

Depending on the initial distribution, they call $\mathcal{F}[\rho]$ the *area flux* if ρ is uniform and call $\mathcal{F}[\rho]$ the *PDF flux* if ρ is the invariant measure π (Eqn (2.3)). For a given set $A \subset D$, the "mass flux into A" is defined as

$$\int_{x\in A} \left(\int_{y\in D\setminus A} P(y, x)\rho(y)\,\mathrm{d}y \right) \mathrm{d}x$$

and "mass flux out of A " (by switching A and its complement set $D\setminus A$) is defined as

$$\begin{aligned} \mathcal{F}_A^- &= \int_{x\in D\setminus A} \left(\int_{y\in A} P(y, x)\rho(y)\,\mathrm{d}y \right) \mathrm{d}x \\ &= \int_{y\in D\setminus A} \left(\int_{x\in A} P(x, y)\rho(x)\,\mathrm{d}x \right) \mathrm{d}y \\ &= \int_{x\in A} \rho(x) \left(\int_{y\in D\setminus A} P(x, y)\,\mathrm{d}y \right) \mathrm{d}x. \end{aligned} \tag{3.3}$$

The quantity $\rho(x)P(x, y)$ was used for x in one basin and y in another basin to investigate where a trajectory is most likely to escape the basin boundary. For a few applications [22], the saddle cycles on the basin boundary usually have the maximal flux across the boundary.

4. Transition Path Theory for discrete map

We first formulate the transition path theory for discrete map. Then we identify the point in the orbit $\boldsymbol{\xi}$ with the highest probability mass of being the last passage position during the A-B transition, which is actually the point with the biggest contributions to the transition rate. To further study the development of the current for the transition probability after emitting the set A, we carry out the pathway analysis and target for the dominant transition paths. The precise definitions of these concepts will be explained soon. We remark that the first

approach based on the transition rate is relatively easy for calculation and quite universal for any situations. The second path-based approach needs a thorough exploration of connected paths based on network theory and could have difficult situations that fail to compare the stochastic instability in a quantitative way due to complexity of pathways, although our logistic map example does not meet with such dilemma and shows a clean result. In addition, the above two approaches may also give two different conclusions since the viewpoints of interpreting and comparing the stochastic instabilities are different.

4.1. **Transition path theory for randomly perturbed discrete map.** The original TPT was formulated for the continuous-time continuous-space Markov process [25, 26, 28]. The TPT for the continuous-time discrete-space Markov process (jump process) was developed in [27], in which a detailed analysis for the pathways on the discrete space is of particular interest. Here we present the method of TPT in the setting of the discrete-time continuous-space Markov process.

The transition path theory does not consider the limit of vanishing noise. It assumes that the stochastic system is ergodic and has a unique invariant measure. The main focus of the TPT is the statistical behaviour of the ensemble of *reactive trajectories* between two arbitrary disjoint sets. Assume that A and B are two disjoint closed subsets of the state space D ($D = [0, 1]$ for our example of the logistic map), each of which is the closure of a nonempty open set. The transition of our interest is from A to B. For a discrete-time homogeneous Markov process $\{X_n : n \in \mathbb{Z}\}$, define the first hitting time after time m and the last hitting time before time m of $A \cup B$ as follows, respectively,

$$\begin{aligned} H^+_{AB}(m) &:= \inf\{n \geq m : X_n \in A \cup B\}, \\ H^-_{AB}(m) &:= \sup\{n \leq m : X_n \in A \cup B\}. \end{aligned} \tag{4.1}$$

Then for a generic trajectory $(X_n)_{n\in\mathbb{Z}}$, the ensemble of A-B **reactive trajectories** is defined to be the collection of pieces of the truncated trajectories: $\{X_n : n \in \mathsf{R}\}$, where $n \in \mathsf{R}$ if and only if

$$X_{H^+_{AB}(n+1)} \in B \quad \text{and} \quad X_{H^-_{AB}(n)} \in A.$$

R is the set of times at which X_n belongs to an A-B reactive trajectory. Refer to Figure 1 for one piece of reactive trajectory extracted from a generic trajectory. The intuition for defining A-B reactive trajectories is that the points on these reactive trajectories will first reach B rather than A and came from A rather than B.

The most important ingredient in the TPT is the probability current for A-B reactive trajectories. For the continuous state space D, we introduce its space-discretized version first:

$$\begin{aligned} \mathsf{J}(x, y, \Delta x, \Delta y) := \lim_{N\to\infty} \frac{1}{2N+1} \sum_{n=N}^{-N} \Bigg(& \mathbf{1}_{[x-\frac{\Delta x}{2}, x+\frac{\Delta x}{2}]}(X_n) \mathbf{1}_{[y-\frac{\Delta y}{2}, y+\frac{\Delta y}{2}]}(X_{n+1}) \\ & \mathbf{1}_A(X_{H^-_{AB}(n)}) \mathbf{1}_B(X_{H^+_{AB}(n+1)}) \Bigg), \end{aligned} \tag{4.2}$$

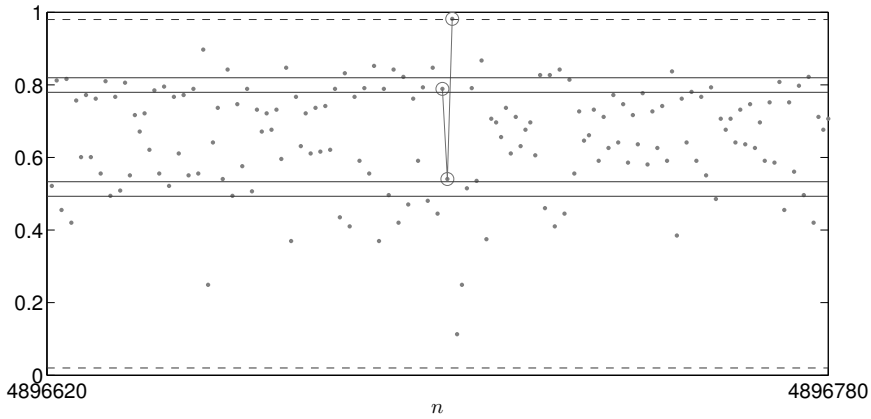

FIGURE 1. A snapshot of a generic trajectory (dots in the plot) and one reactive trajectory (three points circled in the plot) of the randomly perturbed logistic mapobserved in the time interval $[4896620, 4896780]$. The set A is the union of A_1 and A_2 around the periodic points $\boldsymbol{\xi} = (0.5130, 0.7995)$, corresponding to two narrow bands with length $2\delta_a = 0.04$ shown by solid horizontal lines. The bounds of the set B near 0 and 1 are shown in dashed lines. $\alpha = 3.2$, $\sigma = 0.04$.

where $\mathbf{1}_{\{\cdot\}}(\cdot)$ is the indicator function. Then the A-B **reactive probability current** is defined as the following limiting function for x and y in D,

$$J(x, y) := \lim_{\Delta x, \Delta y \to 0} \frac{\mathsf{J}(x, y, \Delta x, \Delta y)}{\Delta x \Delta y}.$$

We sometimes just call J the reactive current whenever the specification of the sets A and B is clear.

The above definition of the reactive current J is based on the time average for an infinitely long generic trajectory. To obtain an ensemble average, we need assume the Markov process $\{X_n\}$ is ergodic, i.e., the unique existence of the invariant probability density such that $\pi(x) = \lim_{N\to\infty} \frac{1}{N} \sum_{n=0}^{N-1} \mathbf{1}_x(X_n)$. Then, (4.2) leads to the following formula of the reactive current

$$J(x, y) = q^-(x)\pi(x)P(x, y)q^+(y), \ x \in D, y \in D. \tag{4.3}$$

where $P(x, y)$ is the transition density function of the Markov process $P(x, y\,\mathrm{d}y = \mathbb{P}[X_{n+1} \in [y, y + \mathrm{d}y)|X_n = x]$, q^+ and q^- are the the forward and backward committor functions, defined as follows, respectively:

$$q^+(x) := \mathbb{P}[X_{H^+_{AB}(0)} \in B|X_0 = x], \ q^-(x) := \mathbb{P}[X_{H^-_{AB}(0)} \in A|X_0 = x].$$

By definition, the committor functions satisfy the following boundary conditions

$$\begin{cases} q^+(x) = 0, \text{ and } \ q^-(x) = 1, & \text{if } x \in A, \\ q^+(x) = 1, \text{ and } \ q^-(x) = 0, & \text{if } x \in B. \end{cases} \tag{4.4}$$

This implies the fact

$$J(x, y) = 0, \text{ when } x \in B, y \in D \text{ or } x \in D, y \in A. \tag{4.5}$$

It is known from [25, 27] that the committor functions satisfy the following Fredholm integral equation for all $x \notin A \cup B$,

$$q^+(x) = \int_D P(x,y)q^+(y)\,\mathrm{d}y,\ x \in D \setminus (A \cup B) \tag{4.6}$$

and

$$q^-(x) = \int_D P^-(x,y)q^-(y)\,\mathrm{d}y,\ x \in D \setminus (A \cup B) \tag{4.7}$$

where

$$P^-(x,y) := \frac{1}{\pi(x)} P(y,x)\pi(y) \tag{4.8}$$

is the transition kernel of the time reversed process $\{X_{-n}\}_{n\in\mathbb{Z}}$. Since the transition kernel P is irreducible in the ergodicity assumption, then the functions $q^+(x)$ and $q^-(x)$ are always strictly positive for any $x \notin A \cup B$.

Remark 1. *Compared with the PDF flux $\pi(x)P(x,y)$ in Section 3.2, the A-B reactive current $J(x,y) = \pi(x)P(x,y)q^-(x)q^+(y)$ in the transition path theory includes the additional global information for the A-B transition of the committor functions. These two quantities are equal only when $x \in A$ and $y \in B$.*

In the next, we shall address two main issues about the methods based on the TPT for the application to the random perturbed discrete map. The first one is the robust calculation of the reactive current function $J(x,y)$ and the second is how to use this reactive current function to analyze the reaction pathways as well as the reaction rate. Based on these developments, we shall carry out the study for the roles of individual points in A and evaluate their stabilities in the content of A-B transitions.

We rewrite the equations (4.7) and (4.8) by introducing $\tilde{q}^-(x) := \pi(x)q^-(x)$, then

$$\tilde{q}^-(x) = \int_D P(y,x)\tilde{q}^-(y)\,\mathrm{d}y,\ x \in D \setminus (A \cup B). \tag{4.9}$$

The boundary condition is $\tilde{q}^-(x) = \pi(x)$ for $x \in A$ and $\tilde{q}^+(x) = 0$ for $x \in B$. Eqn (4.9) has the same form as Eqn (4.6) by transposing the transition kernel P. There are two reasons for introducing $\tilde{q}^-$: (1) the reactive current J, rather than q^- itself, is of more interest in understanding the mechanics of transition and it is not necessary to calculate q^- explicitly in order to obtain J; (2) the numerical method to calculate q^- directly is instable under small noise intensity and this problem can be resolved by calculating $\tilde{q}^-$ instead.

The system (4.9) and (4.6) together with the boundary condition (4.4) can be solved as a linear system after discretizing the spatial domain $D = [0,1]$. $q^+(x)$ and $\tilde{q}^-(x)$ typically exhibit boundary layers or discontinuities at the boundaries of A and B. In our numerical discretisation, the spatial mesh grid is adjusted in a moving mesh style to distribute more points near the boundaries by checking the derivatives $|\nabla q^+|$ and $|\nabla \tilde{q}^-|$ (refer to [10] for details).

Since

$$J(x,y) = q^-(x)\pi(x)P(x,y)q^+(y) = \tilde{q}^-(x)q^+(y)P(x,y), \tag{4.10}$$

then we can see from (4.6) and (4.9) that

$$\int_{y\in D} J(x,y)dy = q^-(x)\pi(x)\int_{y\in D} P(x,y)q^+(y)\,\mathrm{d}y = \tilde{q}^-(x))q^+(x),\ \forall x\notin (A\cup B); \tag{4.11}$$

$$\int_{x\in D} J(x,y)\,\mathrm{d}x = q^+(y)\int_{x\in D} P(x,y)\tilde{q}^-(x)\,\mathrm{d}x = \tilde{q}^-(y)q^+(y),\ \forall y\notin (A\cup B). \tag{4.12}$$

The above quantity on the right hand sides is actually the probability density of reactive trajectories:

$$\pi^{\mathsf{R}}(x) := q^-(x)\pi(x)q^+(x) = \tilde{q}^-(x)q^+(x),\ \forall x\in D\setminus (A\cup B).$$

Under ergodicity condition, this probability density $\pi^{\mathsf{R}}(x)$ corresponds to the following time average: $\pi^{\mathsf{R}}(x)\,\mathrm{d}x = \lim_{N\to\infty}\frac{1}{2N+1}\sum_{-N}^{N}\mathbf{1}_{\mathsf{R}}(n)\mathbf{1}_{[x,x+\,\mathrm{d}x)}(X_n)$. Eqn (4.11) and Eqn (4.12) together show that

$$\int_{y\in D} J(x,y)\,\mathrm{d}y = \int_{y\in D} J(y,x)\,\mathrm{d}y = \pi^{\mathsf{R}}(x),\quad \text{for any } x\in D\setminus (A\cup B). \tag{4.13}$$

So, the reactive current $J(x,y)$ defines a flow at any $x\in D\setminus (A\cup B)$ since the in-flow is equal to the out-flow.

Remark 2. *For the transition kernel $P(x,y)$ based on the discrete map, it is possible that $q^{\pm}(x)$ is continuous only in the open set $D\setminus (A\cup B)$. The one-sided limit from the open set $D\setminus (A\cup B)$ may not equal the boundary value at ∂A or ∂B (note that A and B are closed set and $\partial A\subset A$, $\partial B\subset B$). Thus, there may be a jump discontinuity $q^{\pm}(x)$ at $x\in\partial A\cup\partial B$. Refer to Figure 3 in the next section for the example of logistic map. This means that $J(x,y)$ in (4.10) may also have the jump discontinuities whenever x or y crosses the boundaries at $\partial A\cup\partial B$.*

4.2. **Transition rate and most-probable-last-passage periodic point.** The reactive current J allows us to calculate how frequently the transition occurs from A to B, i.e., the transition rate. The **transition rate** is the average number of transitions from A to B per unit time, defined by

$$\kappa_{AB} := \lim_{N\to\infty}\frac{\#\{\text{transitions from } A \text{ to } B \text{ in } [-N,N]\}}{2N+1}.$$

With the definition of the set R, we can rewrite the above as

$$\kappa_{AB} = \lim_{N\to\infty}\frac{1}{2N+1}\sum_{-N}^{N}\mathbf{1}_A(X_n)\mathbf{1}_{D\setminus A}(X_{n+1})\mathbf{1}_{\mathsf{R}}(n).$$

Remark 3. *When the set A is the union of disjoint compact subsets $A=\cup_{i=1}^{K}A_i$, then it is obvious that the A-B transition rate has the following decomposition*

$$\kappa_{AB} = \sum_{i=1}^{K}\kappa_{A_iB} := \sum_{i=1}^{K}\lim_{N\to\infty}\frac{1}{2N+1}\sum_{-N}^{N}\mathbf{1}_{A_i}(X_n)\mathbf{1}_{D\setminus A}(X_{n+1})\mathbf{1}_{\mathsf{R}}(n),$$

where R still means the A-B transitions. Then the ratio $\dfrac{\kappa_{A_iB}}{\kappa_{AB}}$ is exactly the probability that the reactive trajectory selects the subset A_i to leave the set A during its last stay in the set A.

Using the ergodicity, the transition rate is calculated as follows

$$\begin{aligned}\kappa_{AB} &= \int_{x\in A}\int_{y\in D\setminus A} J(x,y)\,\mathrm{d}y\,\mathrm{d}x = \int_{x\in A}\int_{y\in D} J(x,y)\,\mathrm{d}y\,\mathrm{d}x \\ &= \int_{x\in A} q^-(x)\pi(x)\int_{y\in D} P(x,y)q^+(y)\,\mathrm{d}y\,\mathrm{d}x \\ &= \int_{x\in A}\pi(x)\int_{y\in D} P(x,y)q^+(y)\,\mathrm{d}y\,\mathrm{d}x,\end{aligned} \tag{4.14}$$

where the definition $J(x,y)=\pi(x)P(x,y)q^-(x)q^+(y)$ and the facts that $J(x,y)=0$ for $y\in A$ and $q^-(x)=1$ for $x\in A$ are applied.

From Eqn (4.13), it is clear that

$$\int_{x\in A\cup B}\int_{y\in D} J(x,y)\,\mathrm{d}y\,\mathrm{d}x = \int_{x\in A\cup B}\int_{y\in D} J(y,x)\,\mathrm{d}y\,\mathrm{d}x.$$

By Eqn (4.5), the above equality becomes

$$\int_{x\in A}\int_{y\in D} J(x,y)\,\mathrm{d}y\,\mathrm{d}x = \int_{x\in B}\int_{y\in D} J(y,x)\,\mathrm{d}y\,\mathrm{d}x.$$

Thus, there is an equivalent formula for the transition rate:

$$\kappa_{AB} = \int_{x\in B}\int_{y\in D} J(y,x)\,\mathrm{d}y\,\mathrm{d}x = \int_{y\in B}\int_{x\in D} J(x,y)\,\mathrm{d}x\,\mathrm{d}y. \tag{4.15}$$

The transition rate (4.14) is the total contribution of the reactive current out of A and into B. To distinguish the different points in A, where the reactive current J initiates, we introduce the following two functions $r^-_{AB}(x)$ and $r^+_{AB}(y)$ to represent the local contribution of the reactive current to the reaction rate:

$$r^-_{AB}(x) := \int_{D\setminus A} J(x,y)\,\mathrm{d}y = \int_D J(x,y)\,\mathrm{d}y, \qquad \text{for } x\in A, \tag{4.16}$$

$$r^+_{AB}(y) := \int_{D\setminus B} J(x,y)\,\mathrm{d}x = \int_D J(x,y)\,\mathrm{d}x, \qquad \text{for } y\in B. \tag{4.17}$$

Note that like Eqn (4.14), $r^-_{AB}(x)=\pi(x)\int_{y\in D}P(x,y)q^+(y)\,\mathrm{d}y$, requiring only the forward committor function q^+.

It is easy to see that r^-_{AB} and r^+_{AB} defined in (4.16) and (4.17), after normalization, are known as the reactive exit and reactive entrance distributions in the transition path theory [30,33]. Indeed, by Remark 3, the probability density function of the last passage position on A of a typical reactive trajectory is then given by $\dfrac{r^-_{AB}(x)}{\kappa_{AB}}$ (note $\int_A r^-_{AB}(x)\,\mathrm{d}x=\kappa_{AB}$). Similarly, the probability density function of the first entrance position on B of a typical reactive trajectory is then given by $\dfrac{r^+_{AB}(y)}{\kappa_{AB}}$. We then define the *most-probable-last-passage point* in A as

$$\hat{x} := \arg\max_{x\in A}\frac{r^-_{AB}(x)}{\kappa_{AB}} = \arg\max_{x\in A} r^-_{AB}(x), \tag{4.18}$$

and the *most-probable-first-hitting point* in B as

$$\hat{y} := \arg\max_{y\in B} \frac{r^+_{AB}(y)}{\kappa_{AB}} = \arg\max_{y\in B} \; r^+_{AB}(y). \tag{4.19}$$

Of our particular interest is the most-probable-last-passage point $\hat{x}$ in A. We can think of this point as the most A-B "reactive" point in the set A. In terms of instability due to the noisy perturbation, this point means the least stable location in the set A conditioned on the transitions from A to B.

For the problem of the periodic orbits $\boldsymbol{\xi}$ in the logistic map, the set A is defined as the union of neighbours of the T periodic points $\xi_1, \cdots, \xi_T$, i.e., $A = \bigcup_{1\le i\le T}[\xi_i - \delta_a, \xi_i + \delta_a]$. Since δ_a is small, we can use

$$r^-_{AB}(i) := \frac{1}{2\delta_a}\int_{\xi_i-\delta_a}^{\xi_i+\delta_a} r^-_{AB}(x)\,\mathrm{d}x. \tag{4.20}$$

to represent the contributions to the total flux κ_{AB} from the point ξ_i. We define the **most-probable-last-passage periodic point** (abbreviated to "MPLP") as the point $\xi_{\hat{i}}$ having the maximal value $\{r^-_{AB}(i) : i = 1, \cdots, T\}$. This MPLP is the most unstable periodic point in the sense of transition from the periodic orbit $\boldsymbol{\xi} = (\xi_1, \cdots, \xi_T)$ to the set B.

Remark 4. *The transition rate κ_{AB} is the integration over $x \in A$ for the function*

$$\pi(x)\int_{y\in D\setminus A} P(x,y)q^+(y)\,\mathrm{d}y\,\mathrm{d}x.$$

As mentioned in Remark 1, compared with the PDF flux defined in Eqn (3.3) *(where $\rho = \pi$), the difference between these two formulations is that $q^+(y)$ is multiplied onto $P(x,y)$ here. The inclusion of this forward committor function indicates that in the transition path theory, the object of focus is the A-B reactive trajectories, which have to reach the target set B* before *returning to A. The trajectories counted in the PDF flux* (3.3) *is a much larger set containing those trajectories which failed to reach B and return to A again. So, for the same stochastic system, κ_{AB} is usually much smaller than the quantity $\mathcal{F}^-_A$ in Eqn* (3.3) *unless B is infinitely close to $D \setminus A$.*

The definition of the above MPLP periodic point is associated with the integration of the reactive probability current $J(x,y)$ for all $y \in D \setminus A$. It does not take account of what happens after the reactive current leaves A from the point x. So, it is possible that, once the reactive current flows out of A from the MPLP point $\hat{x}$, the reactive current could quickly diverge and spread out, and as a result, in terms of the transition paths from A to B, different transition paths can carry significantly different values of the reactive currents. We then need to find the dominant ones among all the transition paths connecting A and B. The starting points in A of the dominant transition paths will give our second description of the stochastic instabilities to distinguish the periodic points in $\boldsymbol{\xi}$. Apparently, when the dominant transition paths are not unique due to the complexity of the problem, it is possible that the starting points of these dominant transition paths may lie in multiple subsets A_i for the case of $A = \cup_{i=1}^T A_i$, which means that all these subsets (or the periodic points) are equally instable by this path-based criterion.

4.3. **Competency and maximum competency periodic point.** The analysis of pathways is built on the **effective reactive probability current** $J^+(x,y)$, which is defined by

$$J^+(x,y) := \max(J(x,y) - J(y,x), 0). \tag{4.21}$$

$J^+(x,y)$ is always non-negative and represents the net reactive flux from x to y. We may write

$$J^+(x,y) = \frac{J(x,y) - J(y,x) + |J(x,y) - J(y,x)|}{2}.$$

Then using Eqn (4.13), we obtain

$$\int_{y\in D} J^+(x,y)\,\mathrm{d}y = \int_{y\in D} J^+(y,x)\,\mathrm{d}y, \quad \text{for any } x \in D \setminus (A \cup B).$$

When $y \in A$, $J(x,y) = 0$ and it follows that when $x \in A$, $J^+(x,y) = \max(J(x,y) - J(y,x), 0) = J(x,y)$. So, the formula of the rate (4.14) can also be written in terms of the effective current J^+:

$$\kappa_{AB} = \int_{x\in A, y\in D} J(x,y)\,\mathrm{d}x\,\mathrm{d}y = \int_{x\in A, y\in D} J^+(x,y)\,\mathrm{d}x\,\mathrm{d}y.$$

The effective current $J^+(x,y)$ naturally leads to a series of concepts about the transition paths. These concepts are well described for countable discrete space in [27]. Indeed, in terms of the algorithms, we can divide the continuous domain D into a large number of very fine intervals (much smaller than the widths δ_a and δ_b) and apply the discrete algorithms based on the graph theory described in [27]. The theoretical formulation we give below is for a continuous space domain, and we believe this formulation has its own interest. To represent the functionality of the effective current J^+, we shall use a generic two-dimensional function $f(x,y)$, which is defined on $D \times D$, associated with the given disjoint subsets A and B. This function $f(x,y)$ is an analogue of the weight for an edge from one node x to another y in the graph theory. Clearly, f has to meet the properties that J^+ has. We assume that the triplet (A, B, f) for a compact state space D satisfies the following assumption.

Assumption 1.

(1) *The sets A and B are disjoint nonempty closed subsets of the state space D and $A \cup B \subsetneqq D$;*
(2) *$f(x,y)$ is always non-negative for all $(x,y) \in D \times D$ and*

$$f(x,y) = 0, \text{ if } x \in B, y \in D \text{ or } x \in D, y \in A.$$

(3) *$f(x,x) = 0$, for $x \in D$.*
(4) *For any $x \in D \setminus (A \cup B)$,*

$$\int_{y\in D} f(x,y)\,\mathrm{d}y = \int_{y\in D} f(y,x)\,\mathrm{d}y.$$

(5) *$f(x,y)$ is bounded and piecewise continuous in $D \times D$.*

Definition 1. *Given two disjoint subsets A', B' in D and the triplet (A, B, f) satisfying Assumption 1, for any $n \in \mathbb{N}$, $\boldsymbol{\omega} = (\omega_0, \omega_1, \ldots, \omega_n) \in D \times \cdots \times D$ is called an A'-B'* **transition path** *associated with (A, B, f), if*

(1) $\omega_0 \in A'$, $\omega_n \in B'$;
(2) $f(\omega_i, \omega_{i+1}) > 0$ *for* $0 \le i \le n-1$.

Note that property (2) in Assumption 1 implies that $\omega_i \notin (A \cup B)$ for all $1 \le i \le n-1$.

We actually use $A' = A$ (or $A' \subset A$) and $B' = B$ in most cases. Occasionally, we need a different set B' from B. The following definition of the path competency is from the graph theory.

Definition 2. *We define the* **competency** *of a path* $\boldsymbol{\omega} = (\omega_0, \omega_1, \ldots, \omega_n)$ *as the minimal value of* $f(\omega_i, \omega_{i+1})$ *for all* $0 \le i \le n-1$*, that is,*

$$\mathsf{Cp}(\boldsymbol{\omega}) := \min_{0 \le i \le n-1} f(\omega_i, \omega_{i+1}).$$

Remark 5. *The notion of "competency" defined above is referred to as capacity in the context of the graph theory. However, the terminology "capacity" is also used and plays a significant role in the classical potential theory for stochastic systems which is closely related to the transition path theory. So to avoid confusion, we adopt a different terminology "competency".*

Property (2) in Definition 1 implies that the competency of any A'-B' transition path is always strictly positive.

Definition 3. *With the same assumption in Definition 1, a subset* $\mathcal{C}$ *of the product space* $D \times D$ *is called* A'**-**B' f**-connected***, if there exists at least one* A'-B' *transition path* $\boldsymbol{\omega} = (\omega_0, \omega_1, \ldots, \omega_n)$ *for some* $n \ge 1$*, associated with the triplet* (A, B, f)*, such that every directed edge* (ω_i, ω_{i+1}) *belongs to* $\mathcal{C}$ *for all* $0 \le i \le n-1$.

The collection of all A-B *transition paths with length* n *and all edges contained in the set* $\mathcal{C}$ *is denoted by* $\mathbb{G}_n(\mathcal{C})$. $\mathbb{G}(\mathcal{C}) := \cup_n \mathbb{G}_n(\mathcal{C})$.

We drop out the function f most of the time and simply say the set $\mathcal{C}$ is A'-B' connected. We are particularly interested in the special set $\mathcal{C}$ in the form of the super level set of the function f.

Definition 4. *With the same assumption in Definition 1, define the superlevel set of the function* f *for any non-negative real number* z*,*

$$L_z := \{(x, y) \in D \times D : f(x, y) \ge z\}.$$

The A'**-**B' **competency** *of the function* f*, denoted as* $z^*(A', B')$*, is defined as*

$$z^*(A', B') := \sup \{z \ge 0 : L_z \text{ is } A'\text{-}B' \text{ connected}\}. \tag{4.22}$$

$L_{z^*(A',B')}$ *is call the* **minimal** A'**-**B' **connected superlevel set** *of* f *if the maximizer can be reached:*

$$z^*(A', B') = \max \{z \ge 0 : L_z \text{ is } A'\text{-}B' \text{ connected}\}.$$

As a convention, when A' *and* B' *are not specified,* A' *is* A *and* B' *is* B *by default and we simply say the competency of the function* f*, the minimal connected set and denote* $z^*(A', B')$ *as* z^*.

Remark 6. *The relation between Definition 2 and Definition 4 is that*

$$z^*(A', B') = \sup \{\mathsf{Cp}(\boldsymbol{\omega}) : \boldsymbol{\omega} \text{ is an } A'\text{-}B' \text{ transition path}\}. \tag{4.23}$$

Indeed, if $\boldsymbol{\omega}$ is an A'-B' transition path, then L_z is A'-B' connected for $z \leq \mathsf{Cp}(\boldsymbol{\omega})$; and conversely, if L_z is A'-B' connected, then any A'-B' transition path $\boldsymbol{\omega} = (\omega_0, \omega_1, \cdots, \omega_n)$ with edges contained in L_z must satisfy $f(\omega_i, \omega_{i+1}) \geq z$ for all $0 \leq i \leq n-1$, thus $\mathsf{Cp}(\boldsymbol{\omega}) \geq z$. In particular, all the A-B transition paths with edges in the minimal A-B connected superlevel set L_{z^*} must have the same competency z^* as the function f.

Definition 5. *With the same assumption in Definition 1, let $z^*(A', B')$ be the A'-B' competency of f in Defintion 4, if $L_{z^*(A',B')}$ is A'-B' f-connected, we then call all the A'-B' transition paths with edges in $L_{z^*(A',B')}$ the A'-B'* **dominant transition paths**. *The A-B dominant transition paths are simply called the dominant transition paths.*

In our problem about the periodic orbit $\boldsymbol{\xi} = (\xi_i)_{i=1,\cdots,T}$, the set A is $\cup_{i=1}^{T} A_i$ where $A_i = [\xi_i - \delta_a, \xi_i + \delta_a]$. Note that the following important fact from (4.23),

$$z^*(A, B) = \max_i z^*(A_i, B).$$

Therefore, we propose to make use of the capacities $z^*(A_i, B)$ for $1 \leq i \leq T$ to compare the instability of each ξ_i. The point $\xi_{\hat{i}}$ such that $z^*(A_{\hat{i}}, B) = \max_i z^*(A_i, B)$ is defined as the **maximum competency periodic point** (MCPP). The interpretation of this MCPP is that there exists a transition path emitting from this MCPP (more precisely, its window $A_{\hat{i}}$) whose competency is larger than any transition path emitting from any other periodic point. Thus this MCPP is deemed as the most active (least stable) periodic point in the noise-induced transition from A to B. If this MCPP $\xi_{\hat{i}}$ is unique, then all the dominant transition paths will start from $A_{\hat{i}}$. In case that the maximizers are not unique, the capacities $z^*(A_i, B)$ still can in general give a rank in terms of stochastic instability for all periodic points $\boldsymbol{\xi} = (\xi_i)$.

In the community of graph algorithms and network optimization, the dominant transition path is called the widest path, also known as the bottleneck shortest path or the maximum competency path. There are plenty of practical algorithms to find the widest path [34]. In what follows, we discuss the identification of the A-B competency z^* and the dominant transition paths. The motivation here is not to present the details of the practical implements for discrete state space, but to demonstrate the concepts and the related theoretical properties in the continuos space.

It is easily seen from (4.23) that $z^* > 0$. On the other hand, for $z > \sup_{D\times D} f$, L_z is empty. So, the competency z^* of f satisfies $0 < z^* \leq \sup_{D\times D} f < \infty$. The following properties are obvious: (1) If L_{z_1} is connected, then so is L_{z_2} for any $z_2 < z_1$; (2) L_z is connected for any $0 < z < z^*$; (3) L_z is not connected for any $z > z^*$. So, one can use a binary search algorithm to compute the competency z^* of f within the interval $(0, \sup_{(x,y)\in D\times D} f(x, y)]$. Then the numerical result for z^* is a tiny interval $[z_l^*, z_u^*]$ bracketing the true value z^*. To judge a given set L_z is A-B f-connected or not, we can use the following set-to-set map Φ_z to propagate the set A until reach B if it is reachable. The map Φ_z provides a set-tracking algorithm to search the transition path from A to B. The idea is the analogue of the breadth-first search algorithm. The same procedure is used to test every A_i-B f-connection in order to identify $z^*(A_i, B)$. Actually, since $A = \cup A_i$, the set-tracking is performed in parallel for all A_i.

Definition 6. *For any $z > 0$, we can define the map Φ_z on the collection of all subsets of D by*

$$\Phi_z(C) =: \cup_{x\in C} \{y : (x, y) \in L_z\}, \qquad \forall C \subset D.$$

Denote the compound mapping by

$$\Phi_z^m(C) := \Phi_z(\Phi_z^{m-1}(C))$$

and $\Phi_z^0(C) := C$ by default.

Let

$$N(z) := \min\{n \geq 1 : \Phi_z^n(A) \cap B \neq \emptyset\}$$

be the minimal length of the A-B transition paths in $\mathbb{G}(L_z)$, then $N(z) < \infty$ if and only if L_z is A-B connected.

To avoid the technicality and ease the presentation, we theoretically assume that L_{z^*} is A-B f-connected, i.e., z^* is the maximizer in (4.22). Numerically, we check for z slightly below the numerical value z_l^*, and if for all these z's, they share exactly the same $N(z)$ and the set $\Phi_z^{N(z)}(A) \cap B$ converges as z approaches z_l^*, then we are able to use the obtained numerical value z_l^* as the competency of f defined in (4.22).

4.4. **Dominant transition path and dynamical bottleneck.** Calculating the A_i-B competency, $z^*(A_i, B)$, suffices for quantifying the stochastic instabilities of the periodic points. In the following last part of this section, we further discuss some additional issues about finding the A-B dominant transition paths since such paths can give us more details and insights of the transition mechanism, especially how the periodic points compete in winning the global competency z^*.

First we define a pull back operation.

Definition 7. *Given $z \leq z^*$ and $n \geq N(z)$, let*

$$W_z^{n,n} := \Phi_z^n(A) \cap B,$$

if this set is nonempty. And for $0 \leq i < n$, define recursively,

$$W_z^{n,i} := \{x \in \Phi_z^i(A) : \Phi_z(\{x\}) \cap W_z^{n,i+1} \neq \emptyset\}.$$

For any $\boldsymbol{\omega} = (\omega_0, \omega_1, \cdots, \omega_n)$, define the canonical projection $\pi_i : \boldsymbol{\omega} \mapsto \omega_i$. Then we have the following property about the above set $W_z^{n,i}$.

Proposition 1. *For any $z \in (0, z^*]$, $n \geq N(z)$, and $0 \leq i \leq n$, then*

$$W_z^{n,i} = \pi_i\left(\mathbb{G}_n(L_z)\right),$$

which is to say

(1) *for any $\alpha \in W_z^{n,i}$, there exits a transition path $\boldsymbol{\omega} = (\omega_0, \omega_1, \cdots, \omega_n) \in \mathbb{G}_n(L_z)$ with length n and $\omega_i = \alpha$.*
(2) *for any $\boldsymbol{\omega} = (\omega_0, \omega_1, \cdots, \omega_n) \in \mathbb{G}_n(L_z)$, $\omega_i \in W_z^{n,i}$ for all $0 \leq i \leq n$.*

Proof. (1): Pick up an arbitrary α in $W_z^{n,i}$, let $\omega_i := \alpha$, then there exists a point, denoted as ω_{i+1}, in both $\Phi_z(\{\omega_i\})$ and $W_z^{n,i+1}$. Since $\omega_{i+1} \in W_z^{n,i+1}$, we can inductively find $\omega_j \in W_z^{n,j} \cap \Phi_z(\{\omega_{j-1}\})$ for $i < j \leq n$; in particular, $\omega_n \in W_z^{n,n} \subset B$. Meanwhile, since $\omega_i \in \Phi_z^i(A)$, then there exists an ω_{i-1} such that $\omega_{i-1} \in \Phi_z^{i-1}(A)$ and $\omega_i \in \Phi_z(\{\omega_{i-1}\})$. From $\omega_{i-1} \in \Phi_z^{i-1}(A)$, we similarly have

$\omega_j \in \Phi_z^j(A)$ and $\omega_{j+1} \in \Phi_z(\{\omega_j\})$ for $0 \le j < i$; in particular, $\omega_0 \in \Phi_z^0(A) = A$. Then $\boldsymbol{\omega} := (\omega_0, \cdots, \omega_i, \cdots, \omega_n)$ is the desired transition path.

(2): Let $\boldsymbol{\omega} = (\omega_0, \omega_1, \cdots, \omega_n)$ be a transition path in the set L_z. Then $\omega_0 \in A = \Phi_z^0(A)$. Note that $f(\omega_i, \omega_{i+1}) \ge z$ for all $0 \le i < n$, then $\omega_{i+1} \in \Phi_z(\{\omega_i\})$. In particular, $\omega_1 \in \Phi_z(\{\omega_0\}) \subset \Phi_z^1(A)$, and inductively, we have $\omega_i \in \Phi_z^i(A)$ for $0 \le i \le n$. Since $\omega_n \in B$, thus we have $\omega_n \in W_z^{n,n}$. Then by induction, we obtain from the definition of $W_z^{n,i}$ that $\omega_i \in W_z^{n,i}$ for $0 \le i \le n$. □

Definition 8. *A pair $(x, y) \in D \times D$ is called an A-B* **dynamical bottleneck**, *or* **dynamical bottleneck** *for abbreviation, if $f(x, y) = z^*$ and $(x, y) \in W_{z^*}^{n,i} \times W_{z^*}^{n,i+1}$ for some $n \ge N(z^*)$ and $0 \le i < n$.*

Proposition 2. (1) *If (x, y) is a dynamical bottleneck, then there exists a dominant transition path $\boldsymbol{\omega} = (\omega_0, \cdots, \omega_n)$ in $\mathbb{G}(L_{z^*})$, such that $x = \omega_i$ and $y = \omega_{i+1}$ for some $0 \le i < n$.*

(2) *If for the given set A, B and the function f, the bottleneck is unique, then every dominant transition path contains the bottleneck as one of its edges.*

Proof. (1) From the proof of Proposition 1, we see that if $x \in W_{z^*}^{n,i}$, there must exist an A-$\{x\}$ transition path $(\omega_0, \omega_1, \cdots, \omega_i = x)$ with edges in L_{z^*}, and if $y \in W_{z^*}^{n,i+1}$, there should be a $\{y\}$-B transition path $(\omega_{i+1} = y, \omega_{i+2}, \cdots, \omega_n)$ with edges in L_{z^*}. Since $(x, y) \in L_{z^*}$, then putting together the above two pieces, we obtain $\boldsymbol{\omega} = (\omega_0, \omega_1, \cdots, \omega_i = x, \omega_{i+1} = y, \omega_{i+2}, \cdots, \omega_n)$ is a dominant transition path.

(2) In view of Remark 6, for every dominant transition path $\boldsymbol{\omega} = (\omega_0, \omega_1, \cdots, \omega_n)$ in $\mathbb{G}(L_{z^*})$, we have $\mathsf{Cp}(\boldsymbol{\omega}) = \min_i f(\omega_i, \omega_{i+1}) = z^*$. Let $i^* = \arg\min_i f(\omega_i, \omega_{i+1})$, then $f(\omega_{i^*}, \omega_{i^*+1}) = z^*$. On the other hand, it follows from Proposition 1 that $\omega_{i^*} \in W_{z^*}^{n,i^*}$ and $\omega_{i^*+1} \in W_{z^*}^{n,i^*+1}$. Hence $(\omega_{i^*}, \omega_{i^*+1})$ is a bottleneck by definition. Since the bottleneck is unique, $(\omega_{i^*}, \omega_{i^*+1})$ must be the bottleneck (x, y). □

For the situations that the A-B dynamical bottleneck is unique, which is denoted as $\mathbb{B}(A, B) = (\mathbb{B}^-(A, B), \mathbb{B}^+(A, B))$, we can furthermore recursively investigate how the dominant transition paths leave the set A and reach the bottleneck $\mathbb{B}(A, B)$. For example, we can define the bottleneck $\mathbb{B}(A, \mathbb{B}^-(A, B))$ for the transition from A to $\mathbb{B}^-(A, B)$, i.e., taking $\mathbb{B}^-(A, B)$ as B'. If this bottleneck is also unique, we can continue to trace the nested bottlenecks $\mathbb{B}(A, \mathbb{B}^-(A, \cdots))$ back to some point in the set A. The final point obtained in this recursive way in the set A is just the MCPP we defined before.

4.5. **Comments on two criteria of MPLP and MCPP.** It is normal that our two criteria in Section 4.2 and Section 4.3 can give rise to different results in describing the stochastic instabilities of the same periodic point in regard of different criteria used. The first criterion of looking for MPLP is to compare the total out-flow of the reactive current from a periodic point. The second criterion of looking for MCPP is to compare the competency of the "pipelines" from a periodic point in transporting the reactive current to the destination B. So, it is quite reasonable that the total flow is huge but the competency of each individual pipeline is actually small, or the vice versa. In a nutshell, the MPLP is for the collective behavior of all pipelines while the MCPP is about where the pipeline with the widest bottleneck lies.

5. Application to the random logistic map

We are now in the position to apply the above method based on the TPT to the logistic map for the set A and B specified in Section 2. The first result is for a fixed value $\alpha = 3.2$, at which a stable period-2 orbit exists. We shall show the numerical values of the A-B reactive probability current J and the analysis of the MPLP, MCPP and dominant transition paths. Then, by changing various parameter α and the noise amplitude σ, we study how these quantities change to affect the individual points in one periodic orbit. During the discussion, we also show some validation work for the consistence with the direct simulation and the robustness with respect to δ_a and δ_b.

5.1. **Results for the period-2 case.**

5.1.1. *Basic quantities. (1) invariant measure π:* Pick up $\alpha = 3.2$ as an example first. The stable period-2 orbit in this case is $\boldsymbol{\xi} = (\xi_1, \xi_2) = (0.5130, 0.7995)$. The invariant measure π at $\sigma = 0.04$ is shown in Figure 2a, where the two peaks correspond to the locations of ξ_1 and ξ_2. It is seen that $\pi(\xi_1) < \pi(\xi_2)$, which implies that the periodic point ξ_2 on the right has higher probability at equilibrium. The same result $\pi(\xi_1) < \pi(\xi_2)$ for the two periodic points $\xi_1 < \xi_2$ is observed for all values of α between [3.02, 3.4]. Actually, when α increases in this interval, so does the ratio $\pi(\xi_2)/\pi(\xi_1)$.

Figure 2b shows the invariant measure for a period-3 example at $\alpha = 3.83$. The period-3 orbit is $\boldsymbol{\xi} = (\xi_1, \xi_2, \xi_3) = (0.1561, 0.5047, 0.9574)$. To show the three peaks for this periodic orbit, a smaller $\sigma = 0.008$ is set. It is shown here that the peak at $\xi_3 = 0.9574$ is dominantly large.

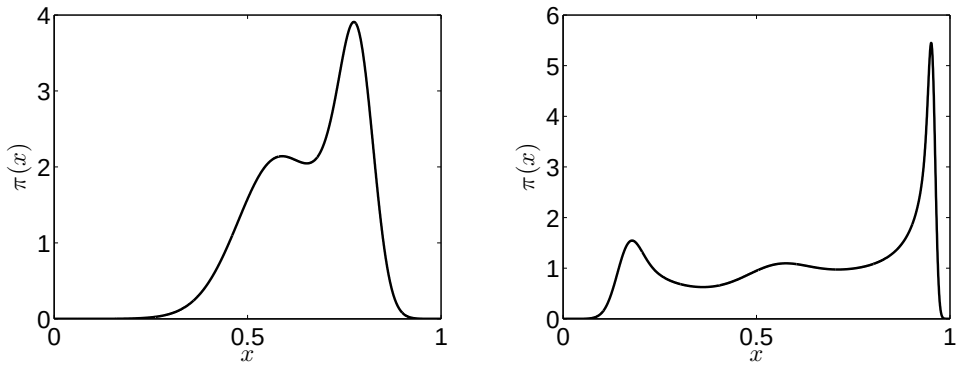

(A) $\pi(x)$ at a period-2 case. (B) $\pi(x)$ at a period-3 case.

Figure 2. The invariant probability density $\pi(x)$ for (A) period-2 case and (B) period-3 case. The parameters are (A) $\alpha = 3.2$, $\sigma = 0.04$, (B) $\alpha = 3.83$, $\sigma = 0.008$.

(2) Committor functions. Choose the sets A and B as in (2.4) and (2.5) with $\delta_a = \delta_b = 0.02$. The forward committor function q^+ and backward committor function q^- at $\sigma = 0.04$ ($\alpha = 3.2$) are plotted in Figure 3 at the logarithmic scale. As a comparison to the solutions obtained from the finite difference scheme for Eqn (4.6) and Eqn (4.7) with 10^4 grid size, shown in the subplot Figure 3a and 3c, the same committor functions in Figure 3b and 3d are calculated from the

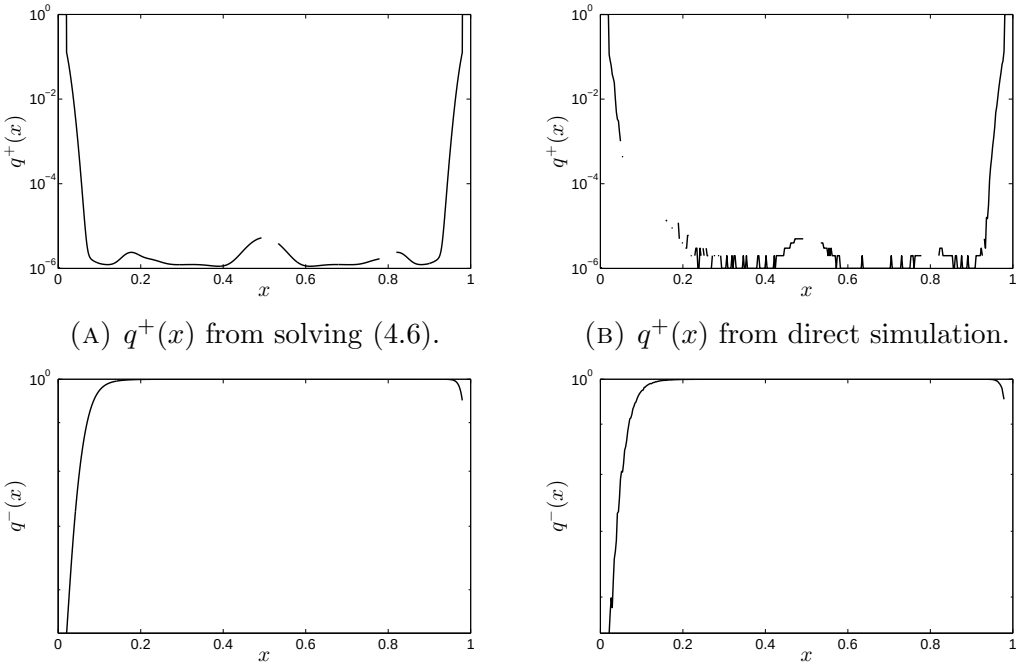

(A) $q^+(x)$ from solving (4.6).

(B) $q^+(x)$ from direct simulation.

(C) $q^-(x)$ from solving (4.7).

(D) $q^-(x)$ from direct simulation.

FIGURE 3. The logarithmic plots of the forward committor function (A, B) and backward committor function (C, D). The parameters are $\alpha = 3.2$, $\sigma = 0.04$, $\delta_a = \delta_b = 0.02$.

statistical average of a long trajectory by brute-force simulation of the random logistic mapping. The total simulation time step is 2×10^{10} (i.e., $N = 10^{10}$ in Eqn (4.14)), during which the number of successful transitions from A to B is 12238. Thus the transition rate obtained from direct simulation is 6.119×10^{-7}. The transition rate calculated from the equation (4.14) is 6.008×10^{-7}.

It should be emphasized that the committor functions are not continuous at the boundary of the sets A and B. The forward committor function does not even change monotonically from 1 to 0. These special features come from the nature of the discrete-time dynamical system.

(3) A-B reactive current. The transition kernel $P(x, y)$ is shown in Figure 4a. Figure 4b plots $\pi(x)P(x, y)$, which is the so-called "PDF flux" in [22]. The A-B reactive current in the TPT for our use, shown in Figure 4c, was calculated from Eqn (4.10) via solving Eqn (4.9) and Eqn (4.6) by finite difference method. Figure 4d is the empirical result from the direct simulation, which shows that our calculation is reliable.

5.1.2. *Stochastic instability comparison at* $\alpha = 3.08$. We fix $\sigma = 0.04$ for the following discussion about the transition mechanism at $\alpha = 3.08$, in which the period-2 orbit is $\boldsymbol{\xi} = (\xi_1, \xi_2) = (0.5696, 0.7551)$.

The first viewpoint of MPLP is to compare the total current out of A, $r^-_{AB}(x) = \int_D J(x, y)\,\mathrm{d}y$ for $x \in A$. The set A of concern is the union $A_1 \cup A_2$, where $A_i = [\xi_i - \delta_a, \xi_i + \delta_a]$, $i = 1, 2$. The set $B = [0, \delta_b] \cup [1 - \delta_b, 1]$. Table 1 shows that δ_a, the width of the set A, has little influence on the result of the transition rate

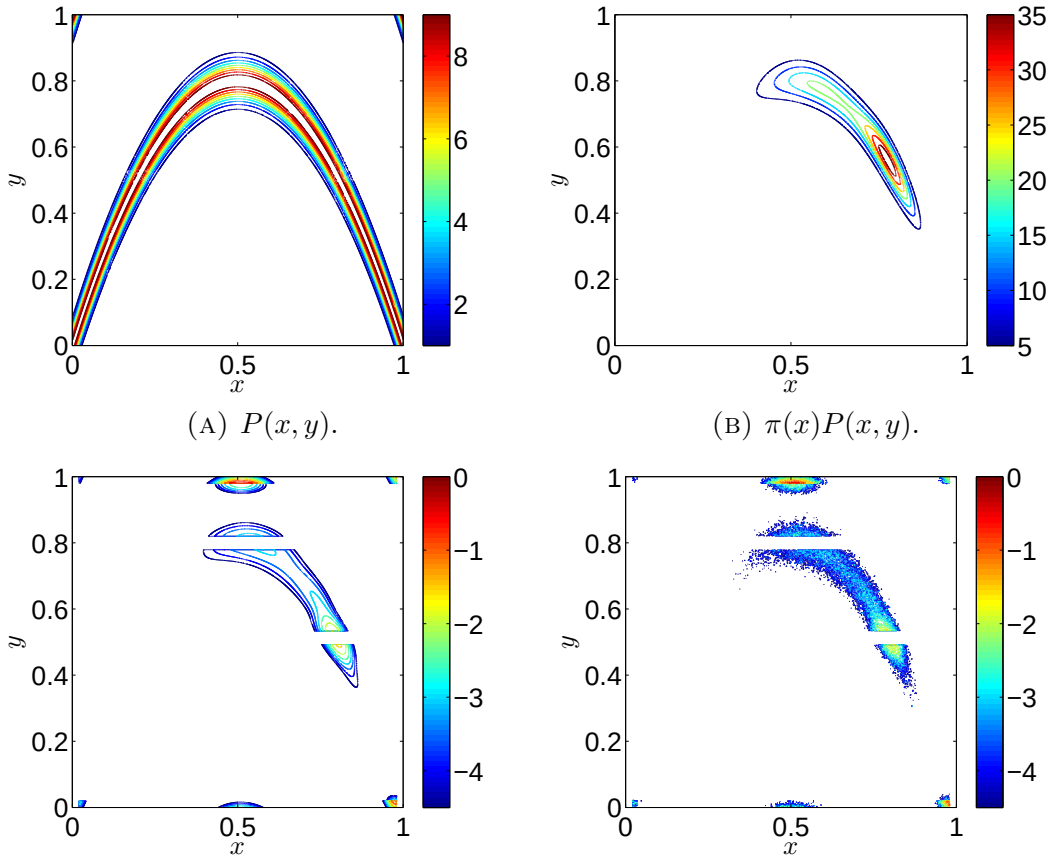

(A) $P(x, y)$.

(B) $\pi(x)P(x, y)$.

(C) $J(x, y)$

(D) empirical $J(x, y)$.

FIGURE 4. The plots of the transition kernel $P(x, y)$, the PDF flux $\pi(x)P(x, y)$ used in [22] and the A-B reactive current $J(x, y) = \pi(x)P(x, y)q^-(x)q^+(y)$. The contour plots for J in subplots (C) and (D) are actually for the value $\log(J(x, y)/M)$ where $M = \max_{x,y\in S} J(x, y)$ for visualization. The parameters are $\alpha = 3.2$, $\sigma = 0.04$, $\delta_a = \delta_b = 0.02$. ($M = 6.5186 \times 10^{-4}$).

k_{AB}	$\delta_a = 0.01$	$\delta_a = 0.015$
$\delta_b = 0.01$	4.6883×10^{-9}	4.6883×10^{-9}
$\delta_b = 0.015$	7.6215×10^{-9}	7.6215×10^{-9}

TABLE 1. Transition rate k_{AB} for different δ_a and δ_b. Here, $\alpha = 3.08$, $\sigma = 0.04$.

κ_{AB}, and δ_b has a slightly more significant influence on κ_{AB}. This observation is expected since the set A is a small neighbourhood of the linearly stable periodic orbit of the logistic map. To test the impact on the MPLP point, we plot in Figure 5 the total current $r^-_{AB}(x)$ for $x \in A_1$ (*left*) and $x \in A_2$ (*right*) for the different widths specified in Table 1. As shown in this figure, the window A_2 where the

periodic point ξ_2 lies carries 30% $\sim$ 50% more reaction current than the window A_1, for various values of δ_a and δ_b. We also tested this result of the MPLP point by varying σ between 0.01 and 0.04, and reached the same conclusion that the second periodic point ξ_2 is the MPLP.

So, our technique based on the relative size of the total current out of the set A robustly identifies the point ξ_2 from the period-2 orbit (ξ_1, ξ_2) as the MPLP. In the sense of the A-B transition events, we can claim that the point ξ_2 is less stable, or more active, under the random perturbation. Note that in terms of the invariant measure, $\pi(\xi_2) > \pi(\xi_1)$. It is ξ_1 that has a smaller equilibrium probability density.

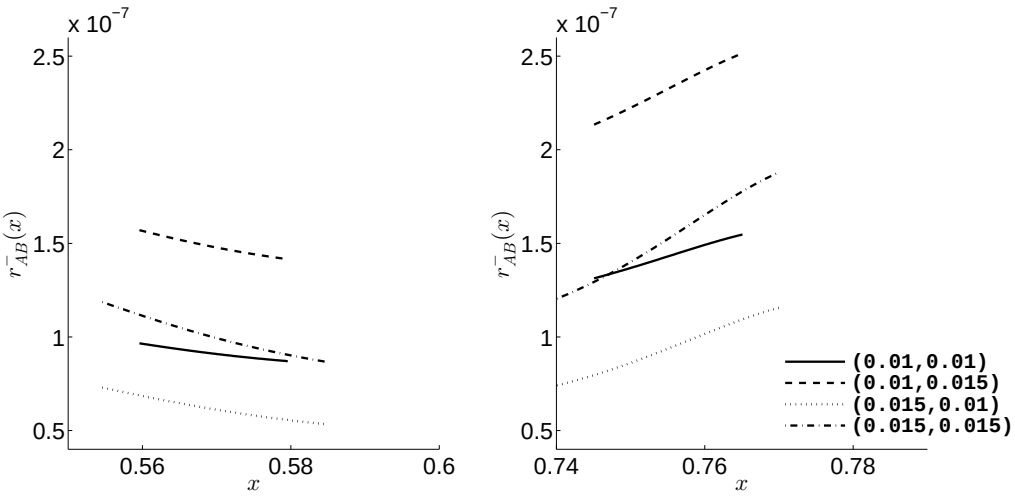

FIGURE 5. $r^-_{AB}(x)$ for x in the union of the sets $A_1 = [\xi_1 - \delta_a, \xi_1 + \delta_a]$(left) and $A_2 = [\xi_2 - \delta_a, \xi_2 + \delta_a]$(right). $\boldsymbol{\xi} = (\xi_1, \xi_2) = (0.5696, 0.7551)$ is the period-2 orbit. $\alpha = 3.08$. $\sigma = 0.04$. The solid line corresponds to $\delta_a = 0.01$, $\delta_b = 0.01$; the dashed line corresponds to $\delta_a = 0.01$, $\delta_b = 0.015$; the dotted line corresponds to $\delta_a = 0.015$, $\delta_b = 0.01$; the dash-dot line corresponds to $\delta_a = 0.015$, $\delta_b = 0.015$.

In the following, we analyze the dynamical bottleneck and dominant transition pathways for this period-2 case. We will restrict to those dominant transition paths with the minimal path lengths $N(z^*)$ to exclude the possible existence of loops. For simplicity, we will omit the $N(z^*)$ in the notation $W_{z^*}^{N(z^*),i}$ and write $W_{z^*}^i$. We choose the window width $\delta_a = \delta_b = 0.01$. After building the effective reactive current $J^+(x, y)$, we found that the A-B competency $z^* \approx 1.98 \times 10^{-6}$ by the binary search between 0 and $M = \max_{D\times D} J^+(x, y)$. $N(z^*)$ is equal to 2. Then, we look for the sequences of the sets $W_{z^*}^i$ for $i = 2, 1, 0$, by using a number of pilot points to explore these sets. The numerical result, up to the accuracy 10^{-4}, shows the following:

$$W_{z^*}^2 = [0.9900, 0.9928] \subset B,$$
$$W_{z^*}^1 = \{0.5331\} \subset D \setminus (A \cup B),$$
$$W_{z^*}^0 = \{0.7651\} \subset A.$$

Then the A-B dynamical bottleneck $\mathbb{B}(A, B)$ is $(0.7651, 0.5331)$. Let 0.5331 be the new set A' and search for the A'-B dynamical bottleneck. Then we obtain

the second dynamical bottleneck $(0.5331, 0.9900)$. Finally, we get the dominant transition path

$$\boldsymbol{\varphi} \approx (\underline{0.7651}, \underline{0.5331}, 0.9900), \text{ at } \sigma = 0.04,$$

where the underlined values correspond to the location of the dynamical bottlenecks. This result of the dominant transition path is unchanged when we changed the grid size between 1.7×10^{-4} and 3.4×10^{-4} in discretizing the space $D = [0, 1]$. We also varied the width δ_a between 0.01 and 0.02 and obtained the same result for the dominant transition path $\boldsymbol{\varphi}$. The first point of the dominant transition path $\boldsymbol{\varphi}$, i.e., the point in $W^0_{z^*}$, lies in the window A_2 for the second periodic point ξ_2. Thus the A-B competency is actually realized by the A_2-B competency. So, we conclude that ξ_2 is also the MCPP. The A-B dominant transition path starts from a boundary point in A_2, followed by a jump to some point on the left but far away from ξ_1 to escape the periodic orbit, and eventually jumps into the set B.

5.2. **Bifurcation diagram for the period-2 case.** It is interesting to see how the above transition mechanisms (MPLP, MCPP, dominant transition paths, etc.) change when the noise amplitude σ or the parameter α changes. The following numerical results show bifurcations for varying parameters, and we will see that the two criteria do not always give the same conclusion.

5.2.1. *change* σ. We still fix $\alpha = 3.08$ but now change the value of the noise amplitude σ between 0.01 and 0.04. Remind that the period-2 orbit is $\boldsymbol{\xi} = (\xi_1, \xi_2) = (0.5696, 0.7551)$.

Figure 6a plots the probability density at ξ_1 and ξ_2 of the last hitting distribution of the transitions from A to B. It shows that ξ_2 always wins ξ_1 as the MPLP for $\sigma \in (0.01, 0.04)$. The dependence of the transition rate κ_{AB} on the noise amplitude σ, in Figure 6b, shows an Arrhenius-like relation.

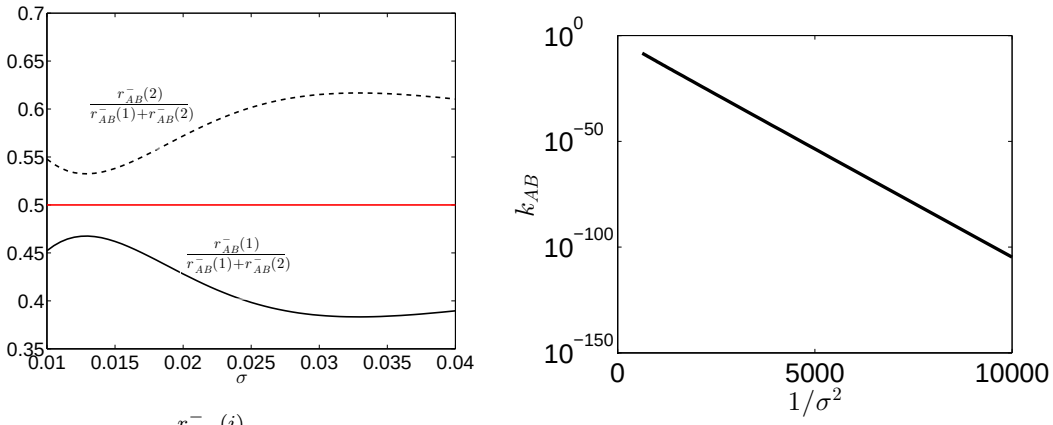

(A) $\frac{r^-_{AB}(i)}{r^-_{AB}(1)+r^-_{AB}(2)}$ versus σ

(B) κ_{AB} versus $1/\sigma^2$.

For the results about the dominant transition paths, the first observation is that the minimal length of the dominant transition paths, $N(z^*)$, grows as σ decreases. For example, at $\sigma = 0.02$, the dominant transition path is $\boldsymbol{\varphi} =$

$(\underline{0.7651}, \underline{0.5269}, 0.9743, 0.0100)$. At $\sigma = 0.014$, the dominant transition path has the minimal length 5:

$$\boldsymbol{\varphi} = (\underline{0.5596}, \underline{0.7761}, 0.5181, 0.9740, 0.0100).$$

At $\sigma = 0.013$, the dominant transition path has the minimal length 6:

$$\boldsymbol{\varphi} = (0.7643, \underline{0.5508}, \underline{0.7818}, 0.5118, 0.9740, 0.0100).$$

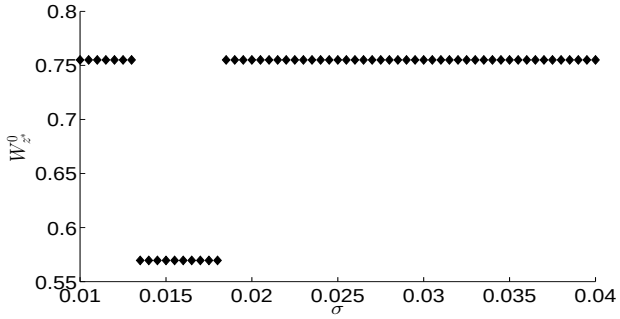

FIGURE 6. The maximum competency periodic point.

When σ varies, Figure 6 plots the MCPP among the choices of the periodic points ξ_1 and ξ_2. This figure shows two critical values of σ: $\sigma_1 \approx 0.0134$ and $\sigma_2 \approx 0.0185$, where ξ_1 and ξ_2 exchange their roles as MCPP.

$\sigma =$	$0.0130 < \sigma_1$	$0.0134 \approx \sigma_1$	$0.0136 > \sigma_1$
$\boldsymbol{\varphi}_1 = (\xi_1, \cdots)$	$\underline{0.5596}$, $\underline{0.7751}$, 0.5196, 0.9740, 0.0100	$\underline{0.5596}$, $\underline{0.7758}$, 0.5186, 0.9740, 0.0100	$\underline{0.5596}$, $\underline{0.7758}$, 0.5186, 0.9740, 0.0100
$J^+(\boldsymbol{\varphi}_1)$	**0.0150**, 0.0165, 0.0242, 0.3753	**0.0053**, 0.0063, 0.0093, 0.1255	**0.0243**, 0.0289, 0.0424, 0.5557
$\boldsymbol{\varphi}_2 = (\xi_2, \cdots)$	0.7644, $\underline{0.5509}$, $\underline{0.7818}$, 0.5119, 0.9740, 0.0100	0.7641, $\underline{0.5513}$, $\underline{0.7818}$, 0.5119, 0.9740 , 0.0100	0.7641, $\underline{0.5516}$, $\underline{0.7818}$, 0.5119, 0.9740, 0.0100
$J^+(\boldsymbol{\varphi}_2)$	0.0230, **0.0152**, 0.0260, 0.0363, 0.3753	0.0079, **0.0053**, 0.0091, 0.0126, 0.1255	0.0357, **0.0240**, 0.0410, 0.0567, 0.5557
$z^* =$	0.0152	0.0053	0.0243
$\boldsymbol{\varphi} =$	$\boldsymbol{\varphi}_2$	$\boldsymbol{\varphi}_1$, $\boldsymbol{\varphi}_2$	$\boldsymbol{\varphi}_1$

TABLE 2. The A-B dominant transition path $\boldsymbol{\varphi}$ and the A-B competency z^* for three values of σ: $\sigma < \sigma_1$, $\sigma = \sigma_1$ and $\sigma > \sigma_1$. $\boldsymbol{\varphi}_1$ and $\boldsymbol{\varphi}_2$ are the A_1-B and A_2-B dominant transition paths respectively. The various dynamical bottlenecks are underlined. Their capacities are marked in bold font at the J^+ row (by multiplying the unit 10^{-58}, 10^{-54} and 10^{-53}, respectively for each column). The A-B competency, z^*, is determined by the maximum of the A_1-B and A_2-B capacities. Note that the periodic points are located at $\boldsymbol{\xi} = (\xi_1, \xi_2) = (0.5696, 0.7551)$ and $\delta_a = \delta_b = 0.01$.

We demonstrate a more detailed analysis at the bifurcation point σ_1 in Table 2 as well as in Figure 7. Table 2 compares the A_i-B dominant transition paths $\boldsymbol{\varphi}_i$, $i = 1, 2$. That is $z^*(A_i, B) = \mathsf{Cp}(\boldsymbol{\varphi}_i)$ for $i = 1, 2$. The A-B dominant transition path $\boldsymbol{\varphi}$ is the path among $\boldsymbol{\varphi}_1$ and $\boldsymbol{\varphi}_2$ with the larger competency. Remind that the competency of a given path $(\varphi_0, \cdots, \varphi_N)$ is calculated as the minimum of the effective currents $J^+(\varphi_n, \varphi_{n+1})$ at each edge $(\varphi_n, \varphi_{n+1})$, which is denoted in bold font in Table 2.

To understand the bifurcation of the MCPP, we need analyze the competition of the two capacities $z^*(A_1, B)$ and $z^*(A_2, B)$, which are further determined by the A_i-B dynamical bottlenecks $\mathbb{B}(A_i, B)$ on the A_i-B dominant transition paths $\boldsymbol{\varphi}_i$ for $i = 1, 2$. The A_1-B dynamical bottleneck is the first step of jump on $\boldsymbol{\varphi}_1$, from the left boundary point of A_1 to a point (located at $0.77 \sim 0.78$) near the right interval A_2. The A_2-B dynamical bottleneck is the second step on $\boldsymbol{\varphi}_2$, corresponding to the jump from a point slightly on the left side of the interval A_1, to a point quite close to one point of the A_1-B dynamical bottleneck. Hence for σ around the value σ_1, both of the A_i-B, $i = 1, 2$ dynamical bottlenecks are the jumps from a region near the left boundary of A_1 (including A_1's left boundary), denoted as I_1 to a region near the right boundary of A_2, denoted as I_2. So, by setting $I_2 = [0.7, 0.82]$ and $I_1 = [0.53, 0.59]$, we investigate the maximum possible reactive current for any given $x \in I_1$: $g(x) := \max_{y \in I_2} J^+(x, y)$ for $x \in I_1$. The maximizer of this function, whether it is equal to the left boundary of A_1 or not, will determine which one of $\boldsymbol{\varphi}_1$ and $\boldsymbol{\varphi}_2$ is the A-B dominant transition path. By plotting the graph of the function g for several σ values around the critical value σ_1 in Figure 8 and rescaling g by its value at the left boundary of A_1, we indeed find that it is the competition of two local maximizers of g that leads to the bifurcation of the dominant transition path from $\boldsymbol{\varphi}_2$ to $\boldsymbol{\varphi}_1$ as σ increasingly passes σ_1 .

The bifurcation at the second critical value σ_2 of the noise amplitude σ is also due to the change of the effective current $J^+(x, y)$, which yields the changes of the MPCC and the dominant transition paths, via the competition of the local maximizers in the interiors and the values at the boundary points of A_1 and A_2 for the function $J^+(x, y)$.

5.2.2. *Change α.* When $\alpha \in [3.02, 3.40]$, the only stable invariant set of the logistic map is the period-2 orbit. We are now interested in how the value of α influences the transition rate and the roles of the individual periodic points. Fix $\sigma = 0.02$

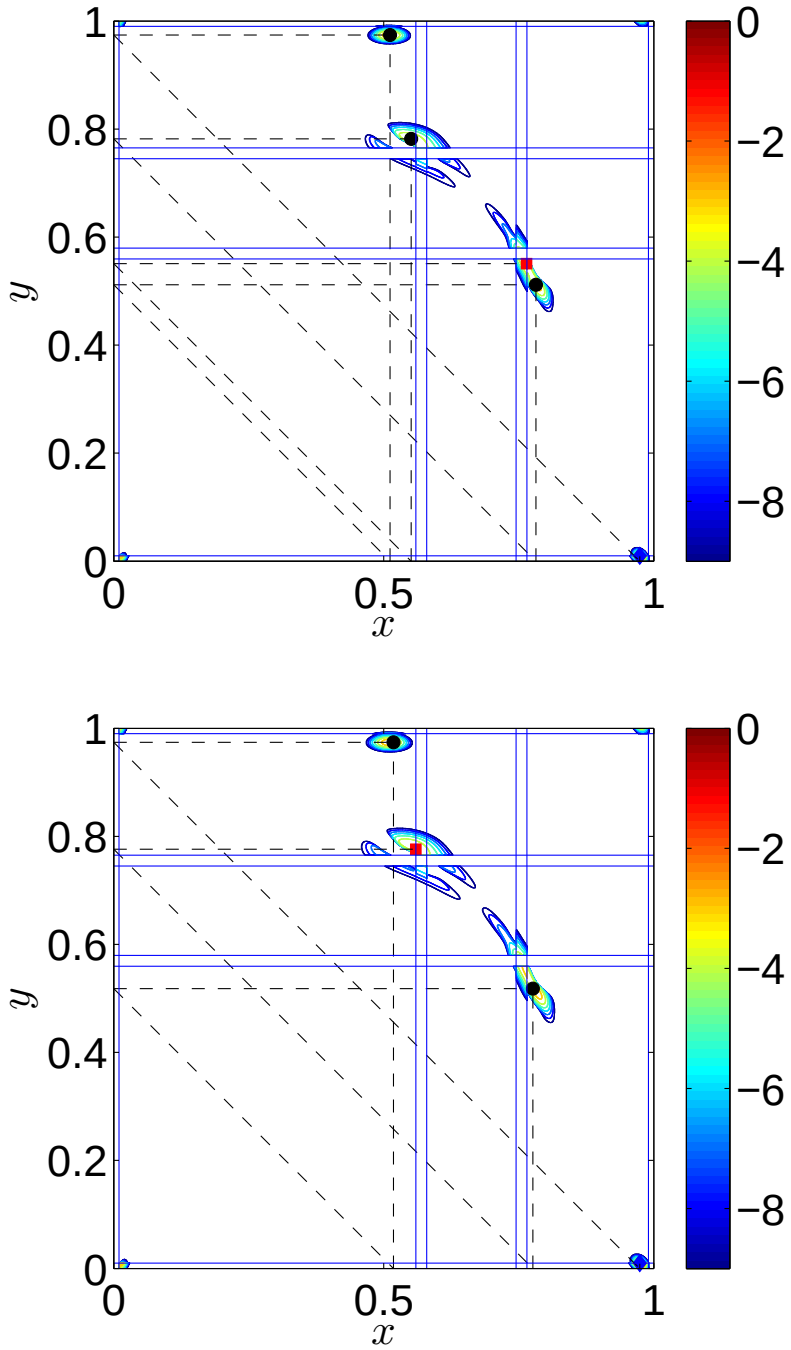

FIGURE 7. This figure visualizes (in form of cobweb plot) the dominant transition path in the contour plot of $\log(J^+/M)$ where $M = \max_{x,y\in D} J^+(x,y)$ ($\alpha = 3.08$, $\delta_a = \delta_b = 0.01$). Top: $\sigma = 0.013$; Bottom: $\sigma = 0.014$. The six vertical and six horizontal straight lines (solid, blue) are the boundaries of A and B. The red and blue dots represent the first and the last edge of the path. The black dots represent all the other edges.

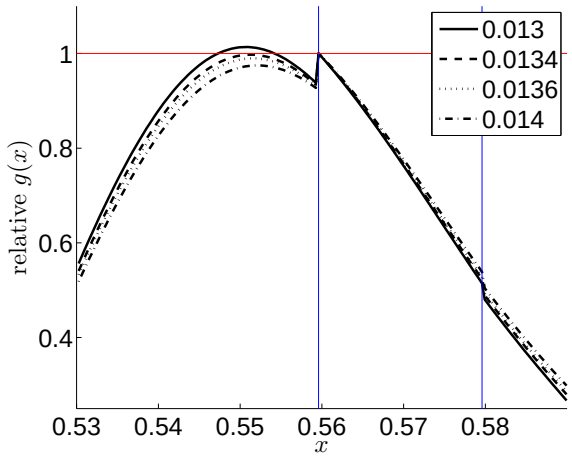

FIGURE 8. The plot of $g(x)/g(\xi_1 - \delta_a)$ near A_1 for the four values of σ from 0.013 and 0.014. Note that g is not continuous at the boundary locations of A_1: $\xi_1 - \delta_a = 0.5596$ and $\xi_1 + \delta_a = 0.5796$, shown as the two vertical lines in this figure.

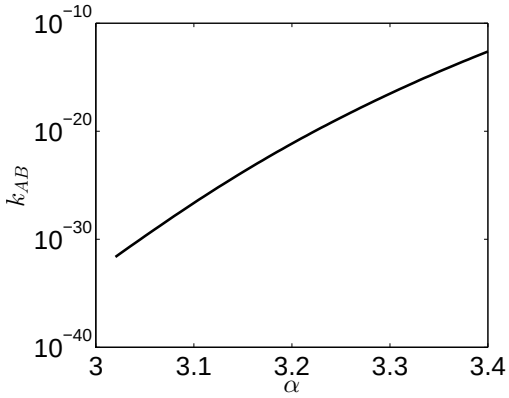

FIGURE 9. κ_{AB} versus α.

and $\delta_a = \delta_b = 0.01$. Figure 9 shows that the transition rate κ_{AB} increases in α and this dependency is nearly exponential. To identify the MPLP between the two periodic points ξ_1 and ξ_2 (ξ_1 is defined to be the smaller one), the probability mass $r^-_{AB}(i)/(r^-_{AB}(1) + r^-_{AB}(2))$ is plotted in Figure 10a. As shown in this figure, ξ_1 is the MPLP only when α is approximately between 3.20 and 3.26. Figure 10b shows the MCPP in dark diamond-shaped dots for each α. For the range of α we investigated here, there are four critical values of α where the MCPP switches between the two periodic points ξ_1 and ξ_2. As explained in Section 4.5, the MPLP and MCPP can be different so the bifurcation points of σ in Figure 10a and 10b are different .

6. DISCUSSION

In conclusion, we have described the method based on the transition path theory, illustrated on the example of the randomly perturbed logistic map, to study

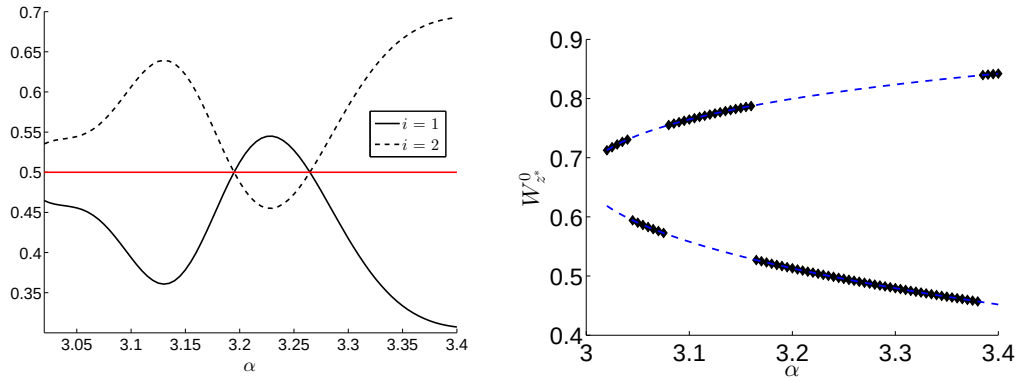

(A) $r^-_{AB}(i)/(r^-_{AB}(1) + r^-_{AB}(2))$ versus α.

(B) The MCPP.

FIGURE 10. The MPLP and the MCPP for $3.02 \leq \alpha \leq 3.40$. $\sigma = 0.02$, $\delta_a = \delta_b = 0.01$. The horizontal straight line in (A) indicates the threshold 0.5. The dashed curves in (B) represent the locations of the two periodic points for each α.

the stochastic instability of the linearly stable periodic orbit in the context of noise-induced transitions. The introduced concepts of most-probable-last-passage point and the maximum competency point are the novel descriptions of the stochastic instability for the linearly stable periodic orbit. We demonstrated the capability of these two proposed perspectives to quantify the stochastic instabilities of the individual periodic point in one periodic orbit. It should be noted that although only the case of period-2 in discrete map was analysed here, our method can also be applied to other types of the set A with more complex structures. In fact, our approach based on the transition path theory is generic to any ergodic stochastic dynamical systems, such as the multiplicative random perturbations, and to the arbitrary nonintersecting closed subsets A and B, such as the stable limit cycles in continuous-time dynamical systems.

REFERENCES

[1] H. A. Karmers, "Brownian motion in a field of force and the diffusion model of chemical reactions," *Physica*, vol. 7, pp. 284–304, 1940.

[2] N. G. van Kampen, *Stochastic Processes in Physics and Chemistry*, vol. 1. North Holland, 2 ed., 1992.

[3] H. Eyring, "The activated complex and the absolute rate of chemical reactions," *Chem. Rev.*, vol. 17, pp. 65–77, 1935.

[4] M. I. Freidlin and A. D. Wentzell, *Random Perturbations of Dynamical Systems*. Grundlehren der mathematischen Wissenschaften, New York: Springer-Verlag, 2 ed., 1998.

[5] B. J. Matkowsky, Z. Schuss, and C. Tier, "Diffusion across characteristic boundaries with critical points," *SIAM J. Appl. Math.*, vol. 43, no. 4, p. 673, 1983.

[6] T. Naeh, M. M. K. osek, B. J. Matkowsky, and Z. Schuss, "A direct approach to the exit problem," *SIAM J. Appl. Math.*, vol. 50, no. 2, pp. 595–627, 1990.

[7] R. S. Maier and D. L. Stein, "Transition-rate theory for nongradient drift fields," *Phys. Rev. E*, vol. 69, no. 26, p. 3691, 1992.

[8] R. S. Maier and D. L. Stein, "Escape problem for irreversible systems," *Phys. Rev. E*, vol. 48, no. 2, pp. 931–938, 1993.

[9] W. E, W. Ren, and E. Vanden-Eijnden, "Minimum action method for the study of rare events," *Comm. Pure Appl. Math.*, vol. 57, pp. 637–656, 2004.

[10] X. Zhou, W. Ren, and W. E, "Adaptive minimum action method for the study of rare events," *J. Chem. Phys.*, vol. 128, no. 10, p. 104111, 2008.
[11] M. Heymann and E. Vanden-Eijnden, "The geometric minimum action method: a least action principle on the space of curves," *Comm. Pure Appl. Math.*, vol. 61, pp. 1052–1117, 2008.
[12] X. Zhou and W. E, "Study of noise-induced transitions in the Lorenz system using the minimum action method," *Comm. Math. Sci.*, vol. 7, pp. 341–355, 2009.
[13] X. Wan, X. Zhou, and W. E, "Study of noise-induced transition and the exploration of the configuration space for the Kuromoto-Sivachinsky equation using the minimum action method," *nonlinearity*, vol. 23, no. 3, 2010.
[14] M. Dykman, P. McClintock, V. Smelyanski, N. Stein, and N. Stocks, "Optimal paths and the prehistory problem for large fluctuations in noise-driven system," *Phys. Rev. Lett.*, vol. 68, no. 18, p. 2718, 1992.
[15] R. L. Kautz, "Activation energy for thermally induced escape from a basin of attraction," *Phys. Rev. A*, vol. 125, pp. 315–319, 1987.
[16] R. L. Kautz, "Thermally induced escape: the principle of minimum available noise energy," *Phys. Rev. A*, vol. 38, no. 4, pp. 2066–2080, 1988.
[17] R. Graham, A. Hamm, and T. Tél, "Nonequilibrium potentials for dynamical systems with fractal attractors or repellers," *Phys. Rev. Lett.*, vol. 66, no. 24, pp. 3089–3092, 1991.
[18] S. Kraut and U. Feudel, "Enhancement of noise-induced escape through the existence of a chaotic saddle," *Phys. Rev. E*, vol. 67, no. 1, p. 015204, 2003.
[19] D. G. Luchinsky and I. A. Khonanov, "Fluctuation-induced escape from the basin of attraction of a quasiattractor," *JETP Letters*, vol. 69, no. 11, pp. 825–830, 1999.
[20] A. N. Silchenko, S. Beri, D. G. Luchinsky, and P. V. E. McClintock, "Fluctuational transitions through a fractal basin boundary," *Phys. Rev. Lett.*, vol. 91, no. 17, p. 174104, 2003.
[21] A. N. Silchenko, S. Beri, D. G. Luchinsky, and P. V. E. McClintock, "Fluctuational transitions across different kinds of fractal basin boundaries," *Phys. Rev. E*, vol. 71, no. 4, p. 046203, 2005.
[22] L. Billings, E. M. Bollt, and I. B. Schwartz, "Phase-space transport of stochastic chaos in population dynamics of virus spread," *Phys. Rev. Lett.*, vol. 88, p. 234101, May 2002.
[23] E. M. Bollt, L. Billings, and I. B. Schwartz, "A manifold independent approach to understanding transport in stochastic dynamical systems," *Phys. D*, vol. 173, no. 34, pp. 153 – 177, 2002.
[24] B. J. Matkowsky and Z. Schuss, "Diffusion across characteristic boundaries," *SIAM J. Appl. Math.*, vol. 42, no. 4, p. 822, 1982.
[25] W. E and E. Vanden-Eijnden, "Towards a theory of transition paths," *J. Stat. Phys*, vol. 123, no. 3, pp. 503–523, 2006.
[26] E. Vanden-Eijnden, "Transition path theory," in *Computer Simulations in Condensed Matter Systems: From Materials to Chemical Biology* (M. Ferrario, G. Ciccotti, and K. Binder, eds.), vol. 1, pp. 453–493, Springer, 2006.
[27] P. Metzner, C. Schütte, and E. Vanden-Eijnden, "Transition path theory for Markov jump processes," *Multiscale Model. Simul.*, vol. 7, p. 11921219, January 2009.
[28] W. E and E. Vanden-Eijnden, "Transition-path theory and path-finding algorithms for the study of rare events," *Annu. Rev. Phys. Chem.*, vol. 61, pp. 391–420, 2010.
[29] F. Noé, C. Schütte, E. Vanden-Eijnden, L. Reich, and T. R. Weikl, "Constructing the equilibrium ensemble of folding pathways from short off-equilibrium simulations," *Proc. Natl. Acad. Sci. U.S.A.*, vol. 106, no. 45, p. 1901119016, 2009.
[30] M. Cameron and E. Vanden-Eijnden, "Flows in complex networks: Theory, algorithms, and application to Lennard-Jones cluster rearrangement," *J. Stat. Phys.*, vol. 156, no. 3, pp. 427–454, 2014.
[31] E. Ott, *Chaos in dynamical systems.* Cambridge University Press, 1993.
[32] W. E, X. Zhou, and X. Cheng, "Subcritical bifurcation in spatially extended systems," *Nonlinearity*, vol. 25, p. 761, 2012.

[33] J. Lu and J. Nolen, "Reactive trajectories and the transition path process," *Probability Theory and Related Fields*, vol. 161, no. 1–2, pp. 195–244, 2015.
[34] R. K. Ahuja, T. L. Magnanti, and J. B. Orlin, *Network Flows: Theory, Algorithms, and Applications*. Upper Saddle River, NJ, USA: Prentice-Hall, Inc., 1993.